NASA TECHNICAL MEMORANDUM

NASA TM X-3348

NASA TM X-3348

MODEL INVESTIGATION OF INLET PLENUM FLOW STRAIGHTENING TECHNIQUES FOR ALTITUDE TEST FACILITY

Stephen M. Riddlebaugh and Heinz G. Linke

Lewis Research Center
Cleveland, Ohio 44135

NATIONAL AERONAUTICS AND SPACE ADMINISTRATION • WASHINGTON, D. C. • FEBRUARY 1976

1. Report No.	2. Government Accession No.	3. Recipient's Catalog No.
NASA TM X-3348		

4. Title and Subtitle	5. Report Date
MODEL INVESTIGATION OF INLET PLENUM FLOW STRAIGHTENING TECHNIQUES FOR ALTITUDE TEST FACILITY	February 1976
	6. Performing Organization Code

7. Author(s)	8. Performing Organization Report No.
Stephen M. Riddlebaugh and Heinz G. Linke	E-8464
	10. Work Unit No.
	505-04

9. Performing Organization Name and Address	11. Contract or Grant No.
Lewis Research Center National Aeronautics and Space Administration Cleveland, Ohio 44135	
	13. Type of Report and Period Covered
12. Sponsoring Agency Name and Address	Technical Memorandum
National Aeronautics and Space Administration Washington, D. C. 20546	14. Sponsoring Agency Code

15. Supplementary Notes

16. Abstract

An investigation was conducted to evaluate and improve the quality of the airflow to be supplied to the engine in altitude test chambers 3 and 4 of the Propulsion Systems Laboratory at the Lewis Research Center. One-twentieth-scale models of the inlet plenum chamber of the two test chambers were used in the investigation to minimize time and cost. It was possible to reduce the velocity spread in the inlet plenum from approximately 100 m/sec (330 ft/sec) to approximately 10 m/sec (30 ft/sec) through the combined use of flow diverters, multiple spaced screens, flow straighteners, and turning vanes.

17. Key Words (Suggested by Author(s))	18. Distribution Statement
Flow straightening Model testing	Unclassified - unlimited STAR Category 09 (rev.)

19. Security Classif. (of this report)	20. Security Classif. (of this page)	21. No. of Pages	22. Price*
Unclassified	Unclassified	31	$3.75

* For sale by the National Technical Information Service, Springfield, Virginia 22161

MODEL INVESTIGATION OF INLET PLENUM FLOW STRAIGHTENING TECHNIQUES FOR ALTITUDE TEST FACILITY

by Stephen M. Riddlebaugh and Heinz G. Linke

Lewis Research Center

SUMMARY

An investigation was conducted to evaluate and improve the quality of the airflow to be supplied to the engine in altitude test chambers 3 and 4 of the Propulsion Systems Laboratory at the Lewis Research Center. One-twentieth-scale models of the inlet plenum chamber of the two test chambers were used in the investigation to minimize time and cost. A variation in flow velocity of approximately 100 meters per second (300 ft/sec) (maximum - minimum) coupled with a large recirculating flow region existed within the inlet plenum upstream of the engine inlet. Mechanical devices that would attenuate the velocity spread, eliminate the recirculation, and straighten the airflow were fitted into the inlet plenum chambers. The velocity difference was reduced to approximately 10 meters per second (30 ft/sec). The pressure drop across these devices at a flow rate simulating a 340-kilogram-per-second (750-lbm/sec) engine flow did not exceed 0.5 newton per square centimeter (0.7 psi).

INTRODUCTION

An experimental scale-model investigation was conducted to evaluate modifications for improving the airflow velocity distribution at the test engine inlet for two new altitude test chambers in the NASA Lewis Propulsion Systems Laboratory. The importance of supplying uniform flow to the engine inlet has been well established as a result of many inlet flow distortion tests. These investigations have shown that engine stall limits are quite sensitive to inlet flow nonuniformities. In addition, nonuniform flow ahead of the engine inlet makes accurate airflow measured extremely difficult.

The flow patterns in the inlet plenums are adversely affected by three factors:

(1) A multiplicity of lines entering and leaving the plenum. There are two sources of air, each with its own inlets into the plenum. The primary source is the facility supply, is preconditioned air. The other source is the atmosphere (for ambient conditions).

The air exits the plenum either through the test section or through a duct controlled by a high-response valve that bypasses the altitude test section. This bypass line is designed to permit rapid engine transients without upsetting the engine inlet and exhaust conditions.

(2) Plenum geometry resulting from space restrictions and the need to tie into existing air supply and exhaust systems. The inlet lines enter the plenum at right angles to the plenum axis, and the inlet lines are closely coupled to the engine inlet bellmouth.

(3) Projected high flow rates. Proposed expansion of the facility air supply and exhaust systems to accommodate testing of jet engines at high flow rates would result in relatively high Mach numbers (up to 0.4) in the inlet lines. These flows would enter the plenums as high-velocity jets.

In designing the inlet plenum modifications, several requirements or ground rules were established:

(1) Any additional hardware should be internal to the inlet plenums. External modifications would be extremely difficult and costly.

(2) The designs should work equally well over a broad range of flow rates without modifications.

(3) Pressure losses across the hardware should be minimal.

(4) At least one screen would have to be incorporated into the designs as a trap for foreign objects.

(5) A honeycomb section would probably have to be incorporated into the design to eliminate swirl.

The test program was divided into two parts. The first part was concerned with cell 3 of the Propulsion Systems Laboratory (PSL 3). Over 250 flow straightening hardware configurations were built and tested in the PSL 3 model. The second part of the test was concerned with adapting the PSL 3 results to the PSL 4 model. About 50 hardware configurations were tested in the PSL 4 model. PSL 4 differs from PSL 3 in that its plenum is two tandem cylindrical sections having different diameters, and the inlets for the conditioned and atmospheric air are offset and at different axial locations instead of at the same axial location.

The tests were conducted primarily at a model flow rate of 0.75 kilogram per second (1.65 lbm/sec). This rate corresponded to a full-scale flow rate of 340 kilograms per second (750 lbm/sec). For selected cases, model flow rates of 0.34 and 1.08 kilograms per second (0.73 and 2.38 lbm/sec) were also investigated. The model Reynolds numbers were above 10^5 so that flow conditions in the model would essentially duplicate those of the full-scale system.

The test results are presented in terms of contour maps of velocity just upstream of the inlet to the bellmouth. In addition, system pressure losses and flow visual observations are also documented.

APPARATUS AND PROCEDURE

Full-Scale PSL Inlet Plenums

The inlet plenum chambers of the PSL 3 and PSL 4 altitude test facilities are sketched in figure 1. Included in the sketches are dimensions indicating the size of the facilities.

Both inlet plenums are characterized by separate inlets for atmospheric air and conditioned air (i. e., air at nonambient pressures and temperatures for altitude and Mach number matching). The twin atmospheric air inlet pipes draw ambient air from a subbasement trench. The conditioned air inlet pipe is tied into the existing facility air supply system. In the PSL 3 plenum, both types of inlet enter at the same axial location; PSL 4 has a stepped plenum in which the conditioned air inlet is upstream of the atmospheric air inlets.

Located about one inlet plenum diameter downstream of the inlets are the bulkheads separating the inlet plenums from the altitude chambers. These bulkheads are represented by broken lines in figure 1. Also indicated are the approximate locations of typical engine-inlet duct installations. The ducts shown would be the size required for a 430-kilogram-per-second (750-lbm/sec) turbofan engine.

The response time of the air supply system is too slow for the system to follow rapid engine transients. Therefore, rapid changes in engine airflow requirements are handled by bypassing varying amounts of air around the altitude chamber through a pipe fitted with a high-response valve. The bypass pipes in both facilities exit the plenum just upstream of the altitude chamber bulkhead. Not shown in the sketches are personnel hatches fitted into each plenum at the same axial location as the bypass line. Access through the hatches prohibited locating many of the flow straightening devices downstream of this point in the plenum.

Test Models

Figure 2 shows cross-sectional schematics of the two models, which were constructed from steel pipe sections and had clear plastic windows for flow visualization. The bellmouth sections and plenum forward and rear bulkheads were constructed from wood. The inner surfaces of the model plenum consisted of several removable cylindrical sections which permitted rapid changes of the flow straightening configurations. The bellmouth between the plenum and the altitude chamber was scaled from a bellmouth for a 340-kilogram-per-second (750-lb/sec) turbofan engine.

Also shown in figure 2 are the locations of the measurement stations. The probe locations at each station are shown in figure 3. Each station contained one or more wall

static taps and a single total-pressure probe that could be manually moved to the locations shown in figure 3. The total-pressure probes were Kiel shielded probes that would give accurate pressure measurements with flow incidence angles up to 30^{o}. All pressure probes were connected to 254-centimeter (100-in.) water manometers.

Airflow was achieved by drawing ambient air through the model into a vacuum exhaust system. Hand valves in the exhaust and bypass lines were used to control flow. Airflow measuring was done at stations 1 and 1A. Airflow calculations were based on a total pressure at the center of the duct, a wall static pressure, ambient temperature, and an assumed flow coefficient. The three inlet flow rate conditions run in the model are listed in table I.

The bulk of the model testing was done at the 0.75-kilogram-per-second (1.65-lbm/sec) flow condition. When the test operating conditions were set up, Mach numbers were matched between the model and the full-scale facility. With kinematic viscosity based on ambient temperature and model pressure levels, model Reynolds numbers at stations 1 and 3 were 5.73×10^{5} and 1.51×10^{5}, respectively, at this flow condition. The corresponding Reynolds numbers in the full-scale facility were 1.20×10^{7} and 3.27×10^{6}, respectively. Model theory states that at Reynolds numbers over 10^{5} viscous effects become essentially independent of Reynolds number. Therefore, Reynolds numbers in the model test were assumed to be of sufficient magnitude to duplicate the flow conditions in the full-scale facility.

TEST CONFIGURATIONS

Over 250 different flow configurations were installed and tested in the two models. They ranged from quite simple to extremely complex systems of ducts, vanes, straighteners, and screen resistances.

The flow straightening configurations covered in this report are summarized in table II. They represent four general approaches to reducing the flow distortion problem. These approaches are the use of (1) series of screen resistances to attenuate the distortion, (2) turning vanes to redirect the flow, (3) ducts to direct the flow upstream to gain additional diffusion lengths, and (4) straightening sections to remove swirl from the flow. Most of the configurations discussed in this report are combinations of all four approaches.

Brief descriptions of the configurations tested and discussed in this report are given in the following paragraphs. These configurations represent the primary variations investigated in reaching the final configuration. Figures 4 to 21 contain sketches of these configurations along with the velocity patterns they produced. Configurations 1 to 12 (figs. 4 to 18) are the hardware configurations fitted to the PSL 3 inlet model.

Configuration 1 (fig. 4) is the PSL 3 inlet plenum model with no flow straightening hardware installed.

Configuration 2 (fig. 5) is the inlet plenum with a single screen installed across it. At least one screen would be installed in the facility as a trap for foreign objects. Consequently, all the PSL 3 model configurations other than configuration 1 contain at least one screen.

Configuration 3 (fig. 6) consists of a turning vane assembly installed in the plenum (along with one screen). The remaining configurations incorporated turning vanes installed in the elbow of the conditioned air supply line as shown in figure 7. Configurations 4 and 5 (figs. 8 and 9) contain various combinations of screens in the inlet plenum.

Configuration 6 (fig. 10) is an attempt to gain additional flow diffusion length in the PSL 3 plenum. The design consists of an annular torus through which the supply air is distributed circumferentially and directed upstream. The flow is then redirected downstream into a conical diffuser formed by the inner wall of the torus.

Configuration 7 (fig. 11) is another attempt to gain additional diffusion length in the plenum by directing the inlet flow upstream. It differs in concept from configuration 6 in that the inlet line is extended into the plenum and directed upstream. The short-radius elbow used in this configuration was a standard pipe elbow with an inside diameter of approximately 10 centimeters (4 in.). The plenum bulkhead had to be moved 2 centimeters upstream to clear the end of the elbow.

Configuration 8, shown in figure 12 without bypass flow and in figure 13 with bypass flow, is configuration 5 with a honeycomb section added to remove swirl from the flow. The honeycomb used in the model test was aircraft structural honeycomb with hexagonal cells. The individual cells had a length-width ratio of about 5 with a length of about 2.5 centimeters (0.88 in.).

Configuration 9 (fig. 14) is configuration 7 with the honeycomb section added.

Configuration 10 (fig. 15) is basically configuration 9 with an elbow of different design fitted to extend the inlet flow line into the inlet plenum. This elbow uses a mitered joint to achieve a right-angle bend and is fitted with internal turning vanes. This design does not require moving the end bulkhead upstream, which would be a major modification to the facility.

Configurations 11 and 12 (figs. 16 and 17) consist of an annular sleeve shielding the bypass flow line fitted to configurations 8 and 10, respectively. As can be seen in the figures, the extraction point for bypass flow is moved downstream of the inlet bellmouth lip to provide more uniform removal of the flow around the circumference of the plenum. Configuration 12 was the configuration ultimately installed in the PSL 3 facility.

The final two configurations discussed in this report are for the PSL 4 inlet plenum. Configuration 13 (fig. 19) is the open inlet plenum. Configuration 14 (figs. 20 and 21) is basically configuration 11 adapted to the PSL 4 inlet geometry. In addition, turning vanes were fitted in the 45° bends of the two atmospheric air supply lines. However, no

vanes were installed in the bends in the conditioned air line. Configuration 14 was ultimately installed in the PSL 4 facility.

RESULTS AND DISCUSSION

PSL 3 With Conditioned Air

Figure 4 shows the velocity profile in the inlet plenum with no flow straightening hardware installed (configuration 1). All the positive flow (flow directed downstream) was crowded into the top portion of the plenum, the remainder of the plenum having zero or reverse flow. The indicated velocity spread at station 3 was 81.2 meters per second, compared with the mean velocity of 10 meters per second.

The zero or recirculating flow regions shown in the figure and in subsequent figures were regions where the measured local total pressures (probe directed upstream) were lower than the wall static pressure. Visual observations of tufts located on the total-pressure probe confirmed reversed and unstable flow in these regions. The local velocities were calculated by using a flow equation rearranged to make velocity a function of the difference between the local total pressure and the wall static pressure. In these recirculating flow regions the local pressure differences were negative and resulted in calculated negative velocities. While the calculated negative velocities cannot be considered to be accurate, they are presented because they do give an indication of the conditions in these regions. It should be pointed out that the recirculating flow regions disappeared as successful flow straightening devices were evolved.

Figure 5 shows the effect of a single 39-percent-open-area screen across the inlet plenum (configuration 2) on the velocity profile at station 3. The positive flow region was slightly larger than that in the open plenum (fig. 4), and the velocity spread was reduced by a factor of nearly 2.

Turning vanes fitted into the plenum (configuration 3, fig. 6) produced inconclusive results. Comparison of the velocity patterns produced by configurations 2 and 3 shows that, while turning vanes increased the size of the positive flow region, the overall velocity spread was unchanged. The velocity spread was reduced by installing additional screens in the plenum, but the screens alone produced a comparable reduction in velocity spread.

A significant contributor to the station 3 distortion pattern when conditioned air was flowing proved to be the elbow in the supply line immediately upstream of the plenum. The flow in the supply line downstream of the elbow (station 2) was greatly distorted compared with the flow upstream of the elbow (station 1), as shown in figures 7(a) and (b). The effect of the flow entering the plenum nonsymmetrically with respect to the plenum axis was to add a large swirl component to the plenum flow pattern.

Turning vanes fitted to the elbow eliminated much of the distortion at station 2 (fig. 7(c)), while reducing the pressure drop across the elbow by a factor of 7. Some improvement in the distortion pattern at station 3 was noted, mostly a reduction in swirl but also some reduction in velocity spread.

Considerable improvement in station 3 velocity profiles was achieved by using turning vanes in the conditioned air supply line combined with a series of screen resistances separated by open spaces. Figures 8 and 9 show the results obtained by using three and four evenly spaced screens of differing open areas (configurations 4 and 5). The station 3 velocity spreads were 9.1 and 4.7 meters per second, respectively, a considerable reduction from those obtained with all previous configurations. The total-pressure loss across each screen averaged 0.14 newton per square centimeter (0.2 psi). No areas of negative velocities or recirculating flow were observed. The flow straightening mechanism was a combination of high flow resistance through the screens and flow mixing in the open spaces between the screens. Choking was not a factor. Four screens were the practical limit for the PSL 3 inlet plenum because of space limitations.

Varying the open areas of the screens produced better results than using the same open area for all screens. Better results were obtained when the screen closest to the inlet was of greater open area than downstream screens. If the open area of the upstream screen was too low, the inlet flow entered the plenum parallel to the screens and jetted along the surface of the upstream screen. When four screens were installed in the plenum (configuration 5), better results were obtained when the first and the fourth screens had a greater open area than the inner two screens. A series of screens separated by open spaces formed a part of all subsequent configurations studied in this test.

Configuration 6 (fig. 10) attempted to gain additional diffusion length in the PSL 3 inlet plenum. The inlet flow was fed into a torus, which discharged upstream. The flow reversed direction and expanded in a conical diffuser formed by the inner wall of the torus. This configuration suffered from a relatively high pressure drop of 0.69 newton per square centimeter (1 psi), possible because of the high-velocity inlet flow impinging on the inner wall of the torus. Tufts indicated that the inlet flow split into streams which jetted around the torus to the top of the plenum, where they entered the conical diffuser. The torus exit screen would probably have to be sized to operate choked in order to improve flow distribution. The effect of operation with a choked screen would be to increase the system pressure loss further.

A much more successful reverse-flow device was created by extending the conditioned air supply line into the inlet plenum and directing its exit upstream. Figure 11 shows a sketch of the final arrangement, configuration 7, and the resulting station 3 velocity profile. The variation in velocity at station 3 was 4.2 meters per second. The pressure drop across the reverse-flow elbow was 0.14 newton per square centimeter (0.2 psi).

While the velocity distortion was nearly eliminated with this configuration, tufts attached to the total-pressure survey probe showed that the flow at station 3 was still not oriented in parallel streamlines. This remaining distortion was corrected by fitting a honeycomb section into the inlet plenum downstream of the other flow straightening hardware. Figures 12 and 14 show configurations 8 and 9, obtained by adding the honeycomb section to configurations 5 and 7, respectively. Velocity profiles deteriorated somewhat, probably because the honeycomb arrested the flow mixing mechanism downstream of the screens and the screen spacing was reduced. The reduced screen spacing was necessary with the honeycomb section because of the facility space limitations.

PSL 3 With Bypass Flow

The flow condition discussed so far did not include bypassing flow around the test section through the bypass flow pipes located as shown in figure 1. It was anticipated that bypassing as much as 40 percent of the inlet flow around the test section would have an adverse effect on the flow profiles at station 3. This proved to be true, as shown in figures 13 and 15.

Figure 13 shows the effect on the station 3 velocity pattern resulting from bypassing 40 percent of the inlet flow with flow straightening configuration 8. Figure 13 can be compared directly with figure 12 for this configuration with no bypass flow. It can be seen that the bypass flow reintroduced a large region of recirculating flow into the inlet plenum. Bypass flow also increased the velocity spread from 11.5 to 25.0 meters per second.

Figure 15 shows the resulting velocity profile when flow is bypassed with a flow straightening configuration incorporating a reverse-flow elbow (configuration 10). As with configuration 8, the bypass flow resulted in a region of recirculating flow at the bottom of the inlet plenum.

The only practical solution found for the bypass flow problem was to fit an annular sleeve into the inlet plenum. The bypass flow was then drawn uniformly from around the circumference of the plenum at a point downstream of the engine inlet bellmouth. Figures 16 (configuration 11) and 17 (configuration 12) illustrate this device as applied to configurations 8 and 10. Velocity profiles both with and without bypass flow are shown. Flow recirculation was eliminated at the expense of increased velocities at station 3 due to reduced flow area.

Configuration 12 (fig. 17) was the flow straightening hardware ultimately built into the full-scale PSL 3 inlet plenum. The resulting velocity spreads at station 3 with and without bypass flow were 7.3 and 8.6 meters per second when conditioned inlet air was used.

PSL 3 With Atmospheric Air

The inlet flow straightening devices tested generally gave slightly better performance when atmospheric air was used than when conditioned air was used. The principal reason for this seemed to be that the atmospheric inlet flow entered the plenum at two points rather than one, which lessened the problem of diffusion.

However, fitting a reverse-flow elbow to the conditioned air inlet line created a blockage in the flow path of the atmospheric air. This is shown in figure 18, which illustrates the performance of configuration 12 when operated with atmospheric inlet flow with and without 40-percent bypass flow. The blockage created a low-velocity region near the center of the station 3 velocity profile. This low-velocity region was small and was not serious. Another problem, a tendency of the inlet flow to jet around the elbow to the top of the duct, was solved by fitting a horizontal deflector to the elbow (fig. 18(a)). This deflector had no effect on operation with the conditioned air supply flow.

PSL 4 With Conditioned Air, Bypass Flow, and Atmospheric Air

Only the performance of the open plenum and the final configuration installed in the full-scale PSL 4 plenum are presented. The intermediate configurations tested were primarily the same as the PSL 3 configurations. Differences in the performance of the two inlet plenums were due to differences in the locations of the conditioned and atmospheric air inlet lines.

The PSL 4 conditioned air supply line is located farther upstream from the altitude chamber inlet than the PSL 3 line (fig. 1). The benefits to the velocity profiles gained from the additional diffusion length were largely cancelled by the impingement of the incoming flow on the 3.7-meter-diameter forward extension of the plenum. Turning vanes were not installed in the conditioned air supply line elbow because the bulkhead extending over the inlet made straightening of the velocity profile at station 2 of questionable value. Also, reverse-flow devices such as found in configurations 6, 10, and 12 were impossible to install.

The PSL 4 atmospheric air inlets are located closer to the test section bulkhead than the PSL 3 inlets, so that there is less room for flow straightening hardware. The atmospheric inlet pipe centers are located closer to the plenum axis than the PSL 3 pipe centers, and the incoming flow had a tendency to jet to the top of the plenum. This was prevented by fitting turning vanes in the elbows where the inlet lines bend inward to join the plenum.

Figure 19 presents the velocity patterns at station 3 in the PSL 4 inlet plenum with no flow straightening hardware installed (configuration 13). Both the conditioned air inlet (fig. 19(b)) and the atmospheric air inlet (fig. 19(c)) results are presented. As in the

PSL 3 inlet with an open plenum (configuration 1), these flow patterns were characterized by a large recirculating region at the bottom of the plenum. The indicated velocity spread at station 3 was 93.4 meters per second with conditioned inlet air and 107.5 meters per second with atmospheric inlet air.

Figure 20 shows configuration 14, which was installed in the full-scale PSL 4 plenum, and the resulting station 3 velocity profile when conditioned supply air was used. The inlet flow impinging on the forward bulkhead produced a low-velocity "shadow" region at station 3. The resulting velocity spread was 15.6 meters per second. When 40 percent of the inlet flow was bypassed, the velocity pattern improved with the velocity spread dropping to 10.3 meters per second.

The performance of configuration 14 when atmospheric inlet air was used and none or 40 percent of the inlet flow was bypassed is shown in figure 21. The velocity spread at station 3 was 12.6 meters per second without bypassed flow and 16.7 meters per second with bypassed flow.

Performance Summarization

The flow straightening performance of the 14 configurations discussed in this report is summarized in figure 22 and in table III. The velocity spreads at station 3 and the pressure drops across the flow straightening devices are presented. It should be noted that the lowest velocity spread did not occur at the highest pressure drop.

Figure 22 relates the velocity spread to the pressure drop across the flow straightening configurations in the PSL 3 model. Only conditioned inlet air data are presented. Each data point is numbered as to configuration.

Three conclusions can be drawn from this figure:

(1) The addition of a fourth screen to the three-screen configuration reduced by a factor of about 2 the velocity spread with no additional loss in pressure (configurations 4 and 5).

(2) The effect on performance of the addition of the honeycomb section can be seen by comparing configurations 5 to 8 and configurations 7 to 9. In both cases, the velocity spread increased noticeably. On the other hand, the pressure drops across the configurations were only slightly affected by the honeycomb.

(3) When the bypass system was used with the bypass sleeve installed (configurations 11 and 12), pressure increased by about 20 percent in both cases; however, the velocity spread was reduced by about 18 to 30 percent below the no-bypass flow conditions.

While the number of points presented in figure 22 is fairly low, they fall in a band of lines defined by the equation

$$\Delta V = \frac{\text{Constant}}{\Delta P^2}$$

where ΔV is the velocity spread at station 3 and ΔP is the pressure drop across the flow straightening configurations, from station 2 to station 3. From the criteria of low pressure drop combined with low velocity spread, the best performing configurations (5 and 12) fall on the line

$$\Delta V = \frac{0.58}{\Delta P^2}$$

Effect of Airflow Rate

The model data presented here were taken at an airflow rate of about 0.75 kilogram per second. A limited amount of data was also taken at flow rates of 0.34 and 1.08 kilograms per second. Two problems encountered at the lower flow rate were (1) difficulty in maintaining a stable flow condition in the model and (2) insensitivity of the manometers to minor velocity changes at station 3. The main problem at the higher flow rate was that of manometer range.

Model performance of 0.34, 0.75, and 1.08 kilograms per second is presented in figure 23. Three configurations are compared at these flow conditions. The data taken at these flow rates indicated that any particular flow straightening configuration produced similar velocity patterns at all three flow rates, although both the velocity spread and the pressure drop increased with flow rate.

SUMMARY OF RESULTS

One-twentieth-scale models of the inlet plenum sections of PSL 3 and PSL 4 altitude test chambers were used to investigate various flow straightening techniques designed to improve the flow distribution. The following results were obtained:

1. A series of uniformly spaced screen resistances prevented flow recirculation from occurring within the inlet plenum and produced relatively uniform velocity profiles. The screens did not choke or produce excessive pressure losses. Better results were obtained if the screen closest to the inlets had greater open area than downstream screens.

2. Additional diffusion length was obtained by extending the conditioned air supply line into the plenum chamber. The extension turned and directed the inlet flow upstream

and discharged it at the forward end of the plenum.

3. A honeycomb grid was required to remove rotational components from the flow. Any distortion pattern present at the honeycomb inlet was transmitted with some modification through the honeycomb.

4. Extracting bypass flow through a single outlet at the bottom of the plenum produced a large region of recirculating flow. This recirculation was prevented by installing an annular sleeve that moved the extraction point downstream of the engine inlet bellmouth. The bypass flow was then drawn from around the circumference of the plenum rather than from a single point.

5. Through the combined use of the various flow control devices, it was possible to reduce the velocity spreads in both inlet plenums from approximately 100 meters per second to 10 to 15 meters per second.

6. Pressure drops across the final PSL 3 and PSL 4 flow straightening configurations averaged 0.31 newton per square centimeter (0.45 psi) when conditioned inlet air was flowing at a rate of 0.75 kilogram per second (1.6 lbm/sec) (equivalent to 340 kg/sec (750 lbm/sec) in the full-scale plenums). When atmospheric inlet air was flowing at the same rate, the pressure drops averaged 0.43 newton per square centimeter (0.62 psi).

7. The flow straightening configurations produced similar velocity patterns at the three flow rates, although the magnitudes of the velocity spread and the pressure drop across the configurations increased as the flow rate increased.

Lewis Research Center,
National Aeronautics and Space Administration,
Cleveland, Ohio, October 16, 1975,
505-04.

TABLE I. - INLET FLOW CONDITIONS

SIMULATED IN PSL 3 AND

PSL 4 INLET MODELS

Mach number at station 1, conditioned air inlet	Model		Full-size facility	
	Equivalent flow rate			
	kg/sec	lbm/sec	kg/sec	lbm/sec
~0.10	0.34	0.73	~140	~300
.25	.75	1.65	~340	~750
~.40	1.08	2.38	~500	~1100

TABLE II. - SUMMARY OF FLOW STRAIGHTENING DEVICES

Test chamber	Configuration	Figure	Number of screens	Location of turning vanes	Type of reverse-flow device	Honeycomb	Bypass flow sleeve	Comments
PSL 3	1	4	0	None	None	No	No	Open plenum
	2	5	1	None	↓	↓	↓	----------
	3	6	1	Inside plenum	↓	↓	↓	----------
	4	8	3	In conditioned air line	↓	↓	↓	----------
	5	9	4	↓	↓	↓	↓	----------
	6	10	4	↓	Cone diffuser	↓	↓	----------
	7	11	4	↓	Round elbow	↓	↓	----------
	8	12, 14	4	↓	None	Yes	↓	----------
	9	13	4	↓	Round elbow	↓	↓	----------
	10	15	3	↓	Mitered elbow	↓	↓	----------
	11	16	4	↓	None	↓	Yes	----------
	12	17, 18	3	↓	Mitered elbow	↓	Yes	Final configuration
PSL 4	13	19	0	None	None	No	No	Open plenum
	14	20, 21	3	In atmospheric air line	None	Yes	Yes	Final configuration

TABLE III. - SUMMARY OF PERFORMANCE OF FLOW STRAIGHTENING DEVICES

[Inlet flow rate, 0.75 kg/sec.]

Test chamber	Configuration	Inlet flow	40-Percent bypass flow	Velocity spread at station 3, m/sec	Pressure drop across flow straighteners, from station 2 to station 3	
					N/cm^2	psi
PSL 3	1	Conditioned	No	[a]81.2	0.01	0.02
	2	↓	↓	[a]47.7	.03	.05
	3			[a]48.3	.18	.26
	4			9.1	.35	.51
	5			4.7	.35	.51
	6			12.4	.64	.93
	7			4.2	.42	.61
	8	Conditioned	No	11.5	0.32	0.46
		Conditioned	Yes	[a]26.0	.30	.44
	9	Conditioned	No	6.2	0.43	0.62
	10	Conditioned	Yes	[a]18.0	.32	.47
	11	Conditioned	No	12.5	0.41	0.59
		Conditioned	Yes	7.8	.49	.71
	12	Conditioned	No	8.6	0.26	0.37
		Conditioned	Yes	7.3	.32	.46
		Atmospheric	No	14.6	0.43	0.62
		Atmospheric	Yes	18.9	.50	.72
PSL 4	13	Conditioned	No	[a]93.4	~0	0.72
		Atmospheric	No	[a]107.5	~0	.72
	14	Conditioned	No	15.6	0.31	0.45
		Conditioned	Yes	10.3	.31	.45
		Atmospheric	No	12.6	0.42	0.61
		Atmospheric	Yes	16.7	.42	.61

[a]Based on estimated negative velocities.

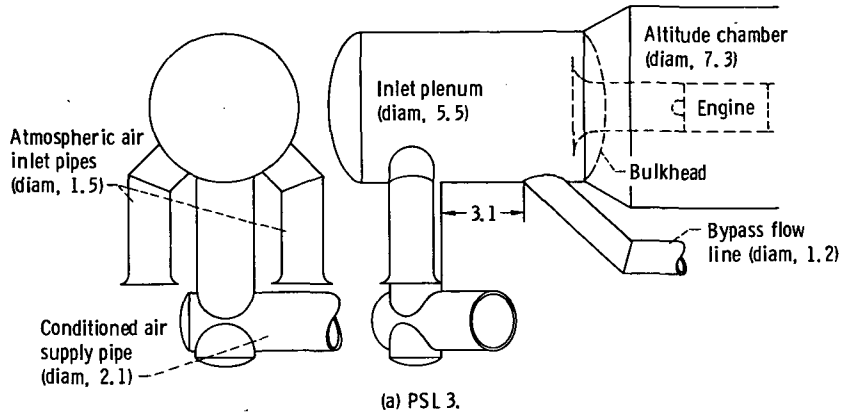

(a) PSL 3.

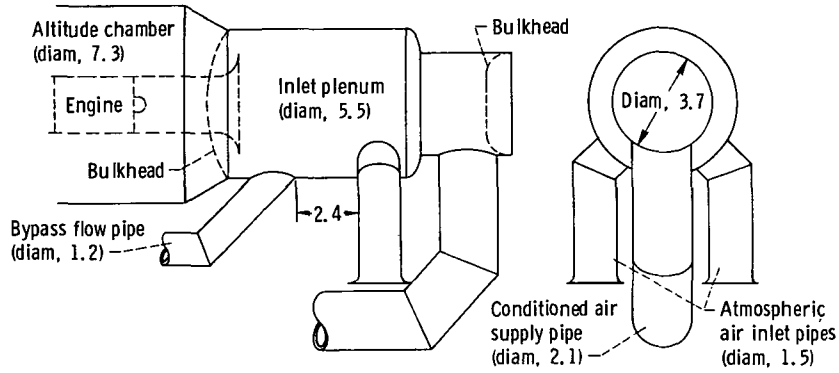

(b) PSL 4.

Figure 1. - Schematics of inlet plenum chambers. (Dimensions in meters.)

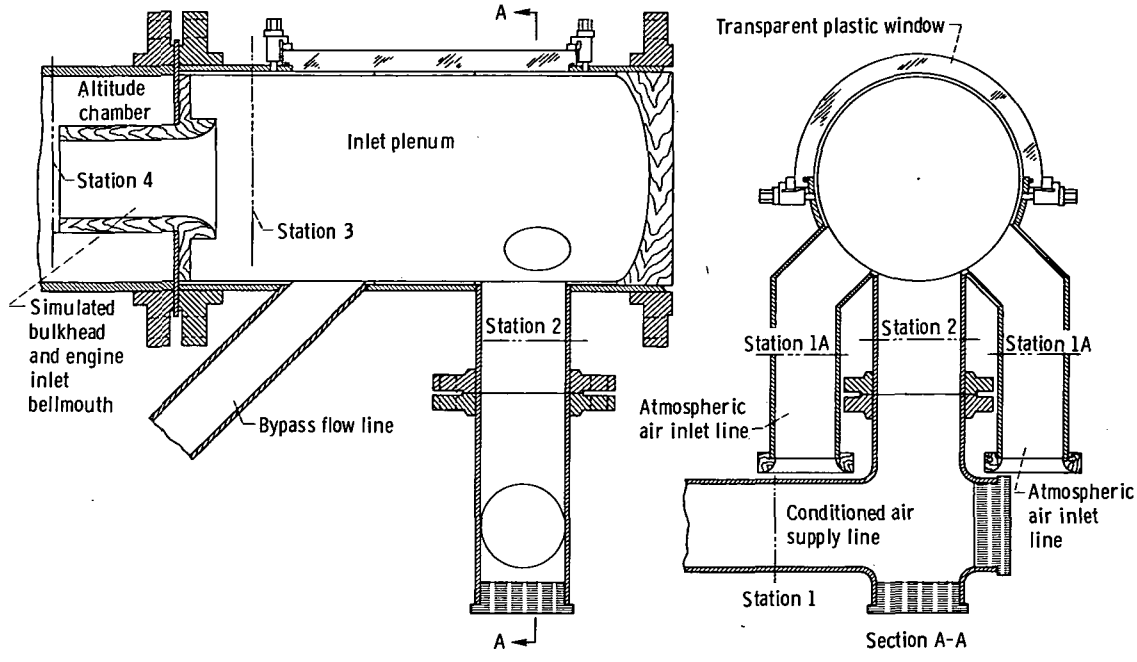

(a) PSL 3.

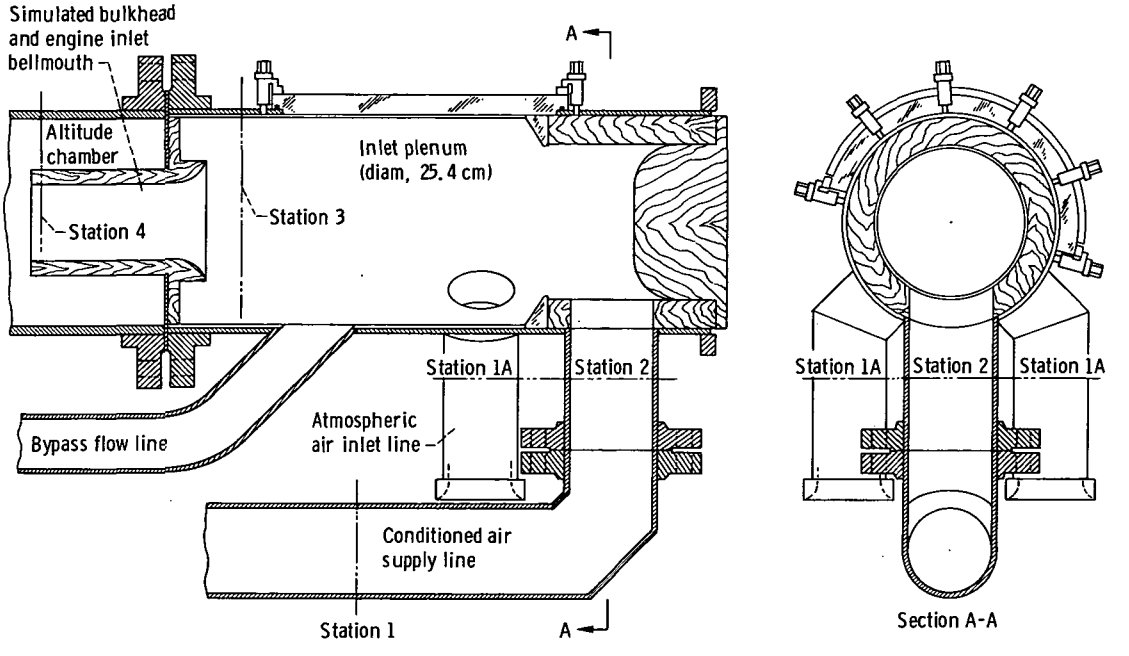

(b) PSL 4.

Figure 2. - Sectional views of one-twentieth-scale model inlet plenums.

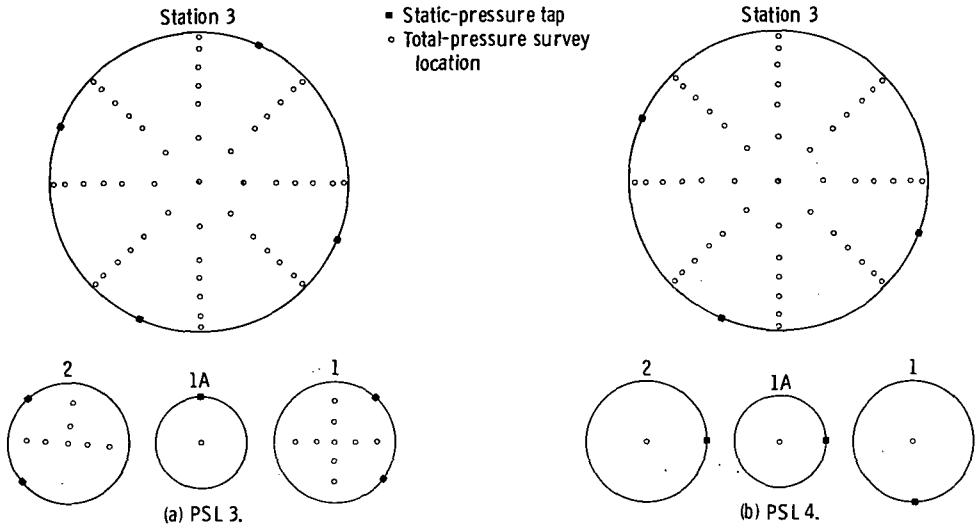

Figure 3. - Locations of model inlet instrumentation.

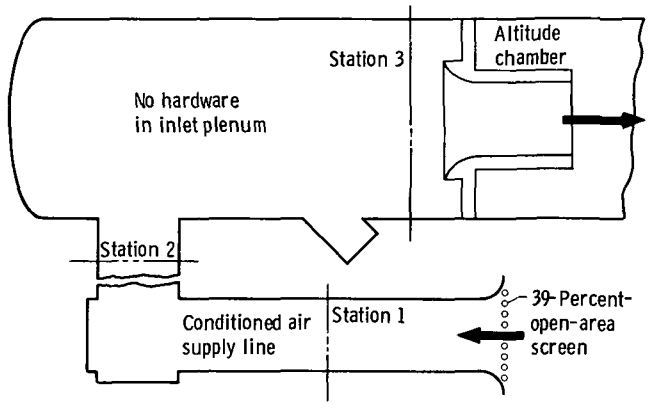

(a) Schematic of configuration 1.

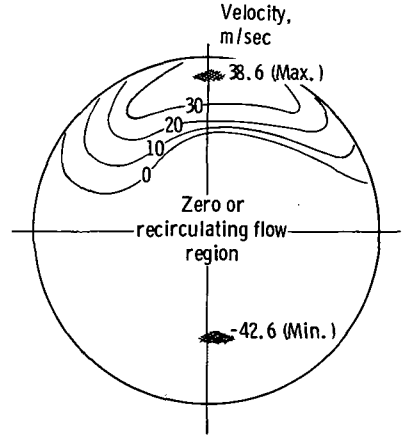

(b) Station 3 velocity pattern, looking downstream; velocity spread, 81.2 meters per second (based on estimated negative velocities).

Figure 4. - Schematic and performance of configuration 1 in PSL 3 inlet model.

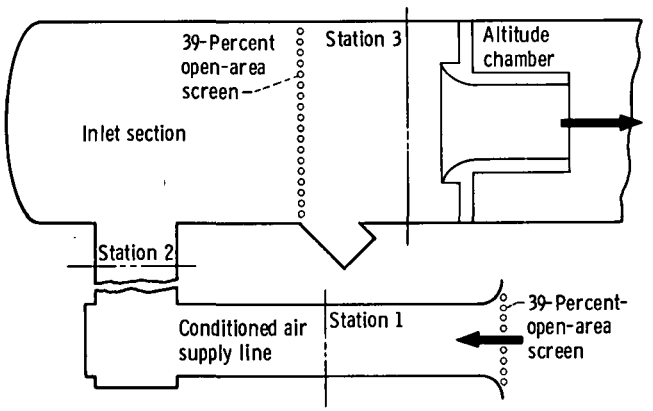

(a) Schematic of configuration 2.

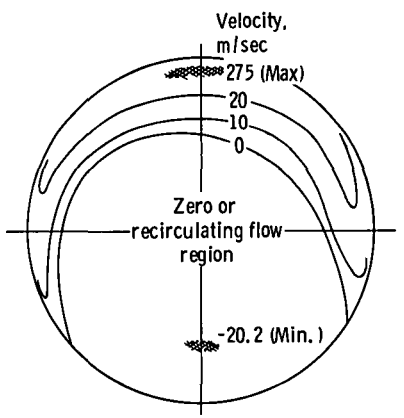

(b) Station 3 velocity pattern looking downstream; velocity spread, 47.7 meters per second (Based on estimated negative velocities).

Figure 5. - Schematic and performance of configuration 2 in PSL 3 inlet model.

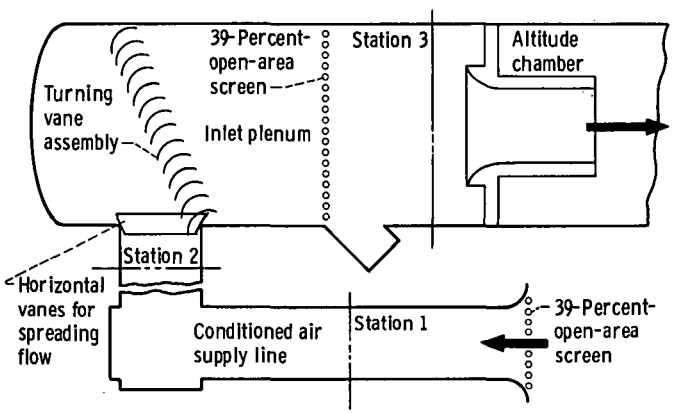

(a) Schematic of configuration 3.

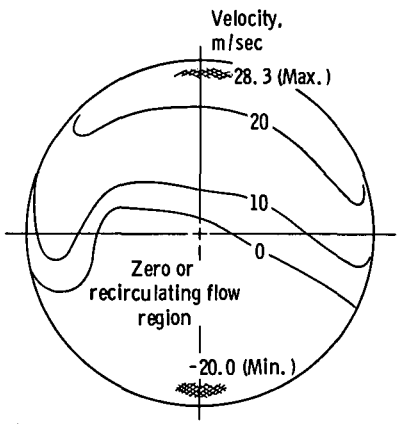

(b) Station 3 velocity pattern looking downstream; velocity spread, 48.3 meters per second (Based on estimated negative velocities).

Figure 6. - Schematic and performance of configuration 3 in PSL 3 inlet model.

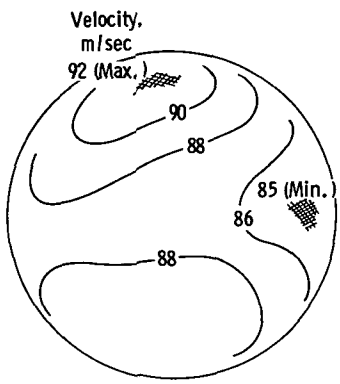

(a) Station 1 velocity pattern, looking downstream.

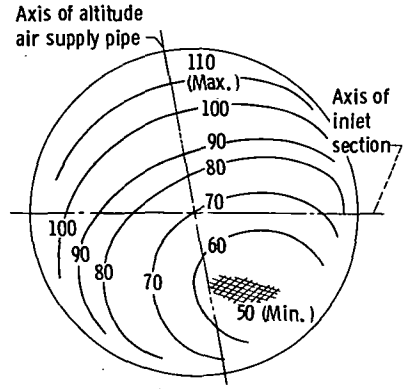

(b) Station 2 velocity pattern, without looking downstream, turning vanes in elbow.

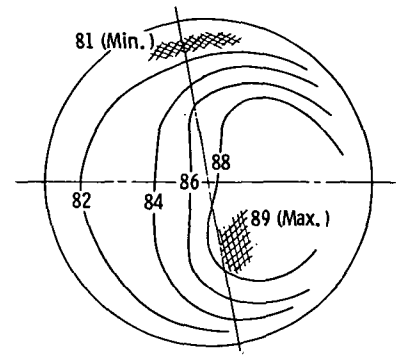

(c) Station 2 velocity pattern, looking downstream, with turning vanes in elbow.

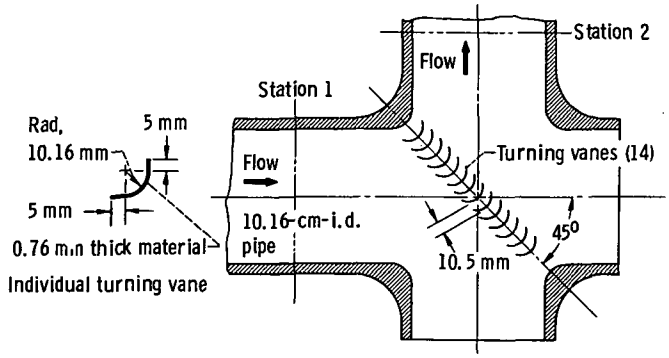

(d) Sketch of turning vane installation in elbow of conditioned air supply line.

Figure 7. - Effects of installation of turning vanes in conditioned air supply line of PSL 3 inlet model. Velocity patterns taken at flow rate of 0.75 kilogram per second (1.65 lbm/sec).

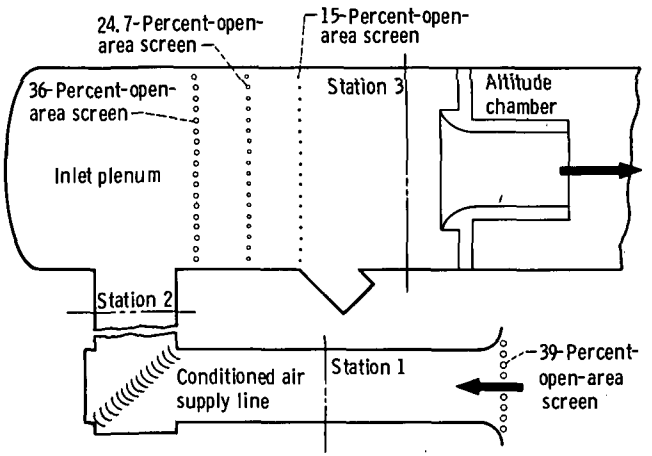

(a) Schematic of configuration 4.

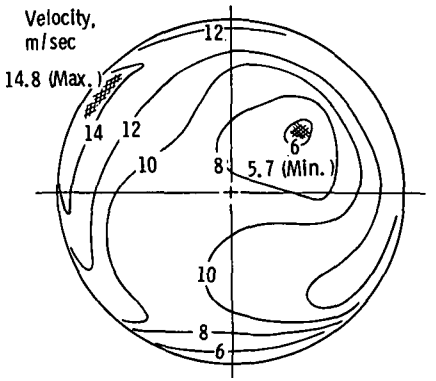

(b) Station 3 velocity pattern, looking downstream; velocity spread, 9.1 meters per second.

Figure 8. - Schematic and performance of configuration 4 in PSL 3 inlet model.

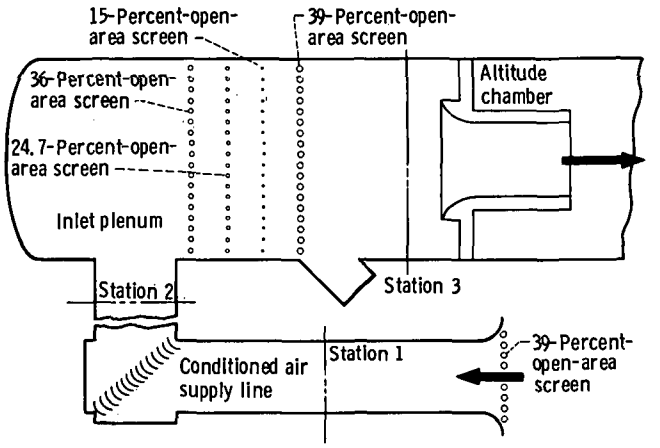

(a) Schematic of configuration 5.

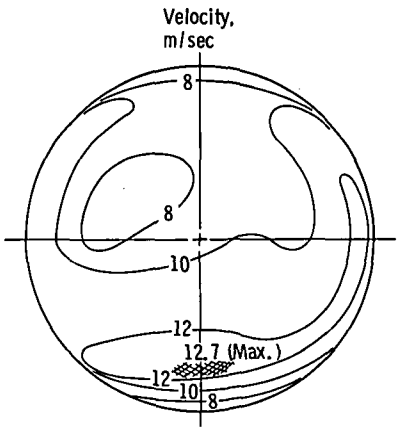

(b) Station 3 velocity pattern, looking downstream; velocity spread, 4.7 meters per second.

Figure 9. - Schematic and performance of configuration 5 in PSL 3 inlet model.

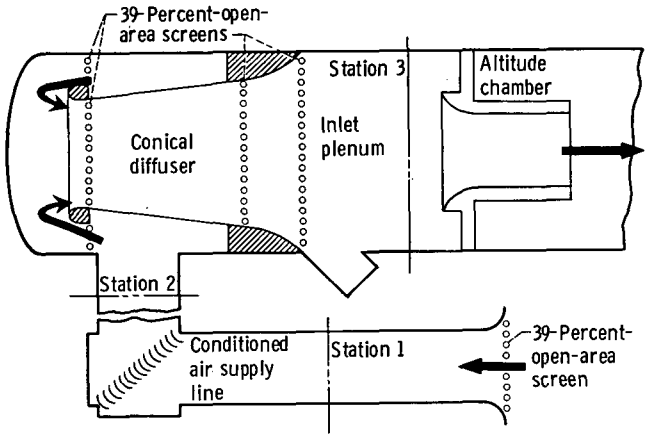

(a) Schematic of configuration 6.

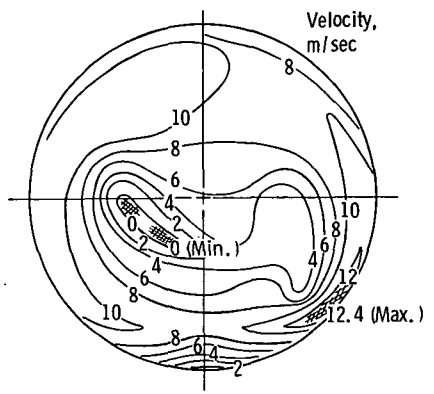

(b) Station 3 velocity pattern, looking downstream; velocity spread, 12.4 meters per second.

Figure 10. - Schematic and performance of configuration 6 in PSL 3 inlet model.

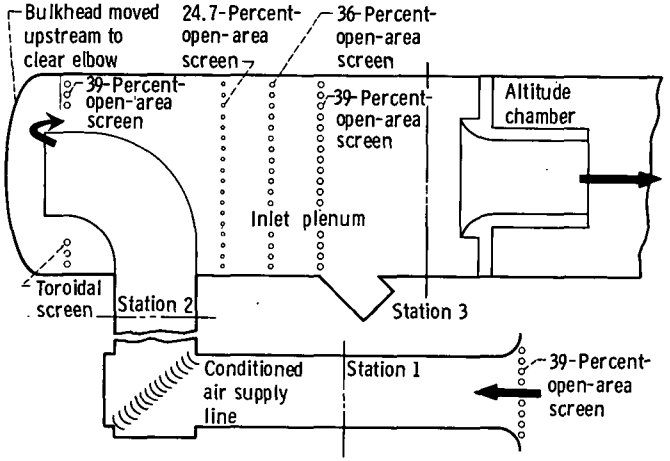

(a) Schematic of configuration 7.

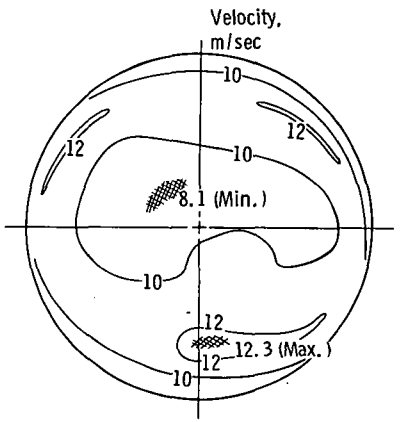

(b) Station 3 velocity pattern, looking downstream; velocity spread, 4.2 meters per second.

Figure 11. - Schematic and performance of configuration 7 in PSL 3 inlet model.

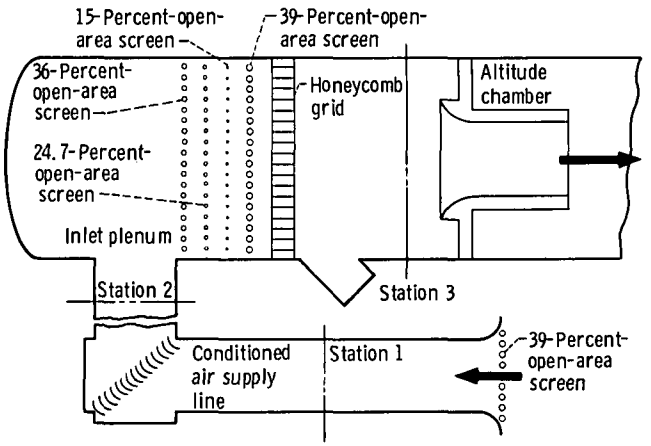

(a) Schematic of configuration 8.

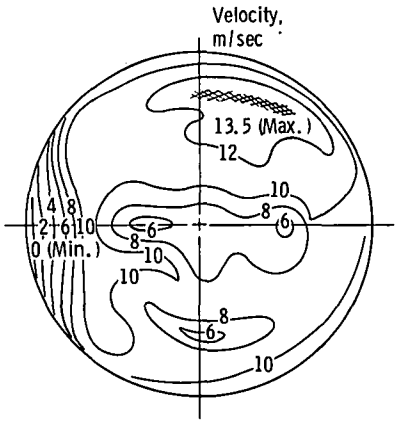

(b) Station 3 velocity pattern, looking downstream; velocity spread, 21.1 meters per second.

Figure 12. - Schematic and performance of configuration 8 in PSL 3 inlet model.

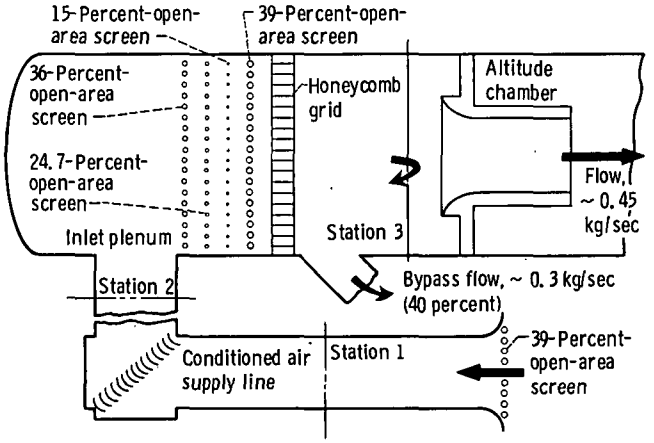

(a) Schematic of configuration 8.

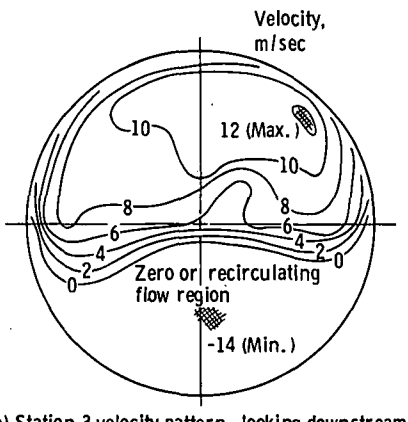

(b) Station 3 velocity pattern, looking downstream; velocity spread, 26.0 meters per second (based on estimated negative velocities).

Figure 13. - Schematic and performance of configuration 8 in PSL 3 inlet model with bypass flow.

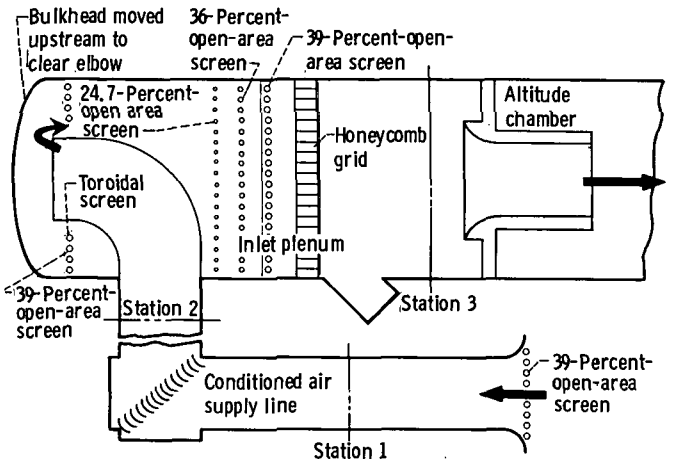

(a) Schematic of configuration 9.

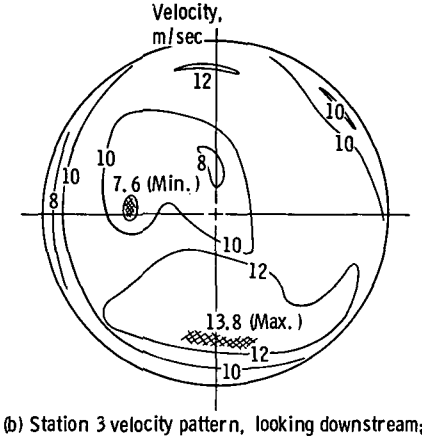

(b) Station 3 velocity pattern, looking downstream; velocity spread, 6.2 meters per second.

Figure 14. - Schematic and performance of configuration 9 in PSL 3 inlet model.

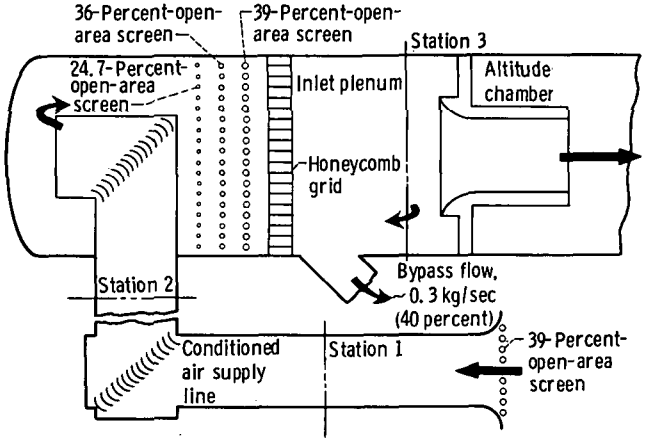

(a) Schematic of configuration 10.

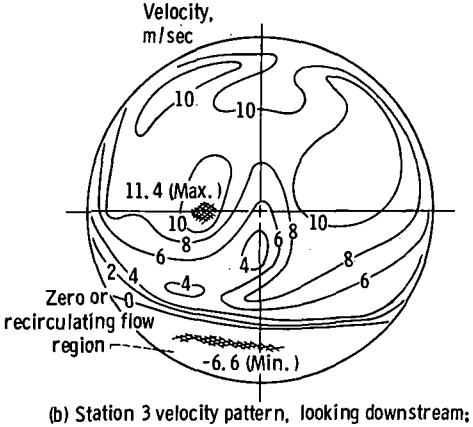

(b) Station 3 velocity pattern, looking downstream; velocity spread, 18 meters per second. (based on estimated negative velocities).

Figure 15. - Schematic and performance of configuration 10 in PSL 3 inlet model with bypass flow.

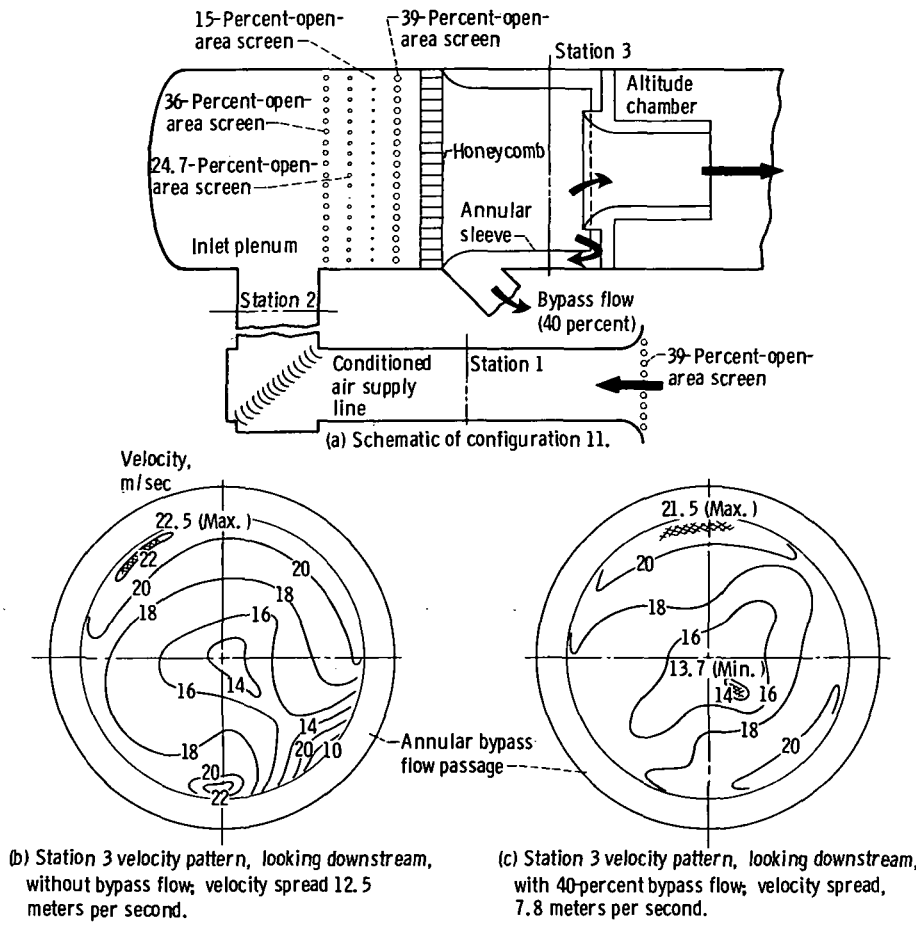

(b) Station 3 velocity pattern, looking downstream, without bypass flow; velocity spread 12.5 meters per second.

(c) Station 3 velocity pattern, looking downstream, with 40-percent bypass flow; velocity spread, 7.8 meters per second.

Figure 16. - Schematic and performance of configuration 11 in PSL 3 inlet model.

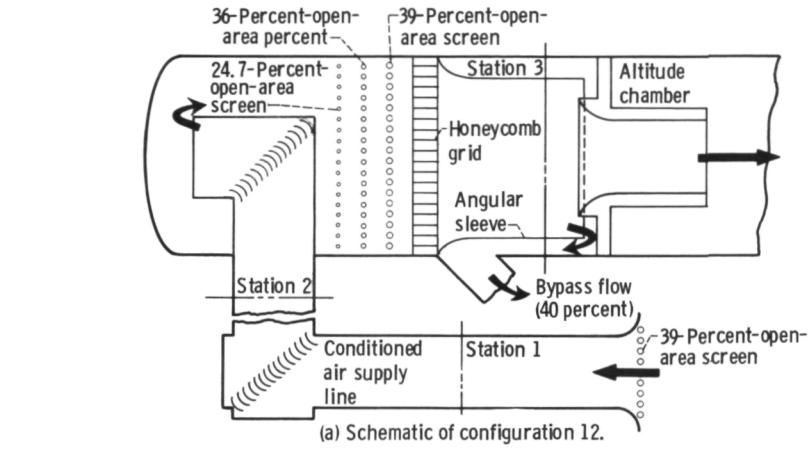

(a) Schematic of configuration 12.

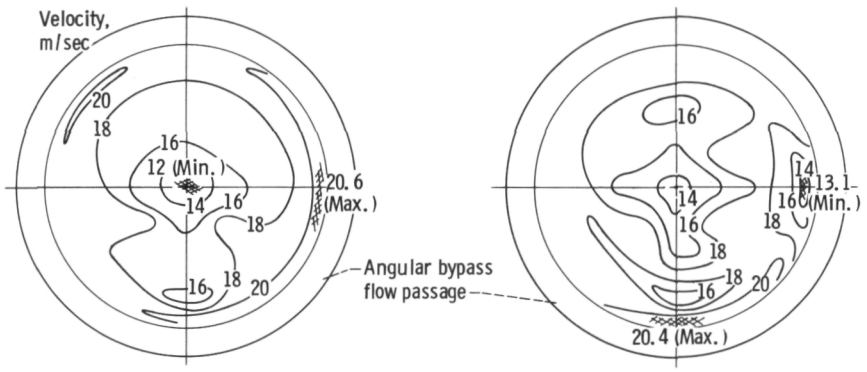

(b) Station 3 velocity pattern, looking downstream, without bypass flow; velocity spread, 8.6 meters per second.

(c) Station 3 velocity pattern, looking downstream, with 40-percent bypass flow; velocity spread, 7.3 meters per second.

Figure 17. - Schematic and performance of configuration 12 in PSL 3 inlet model.

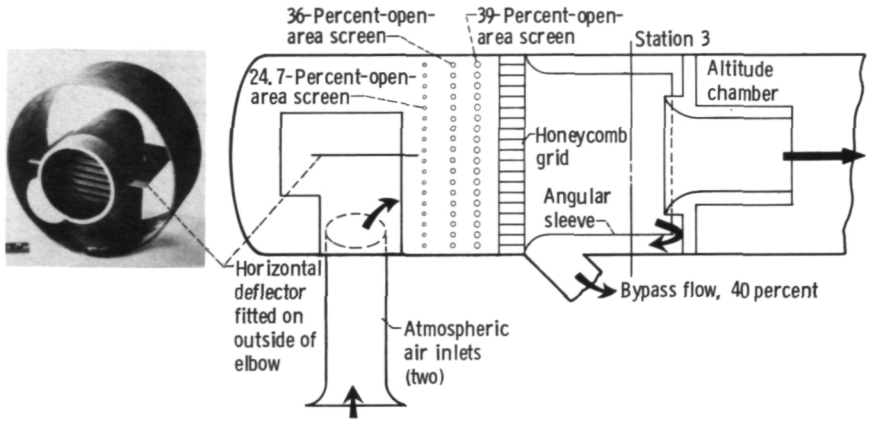

(a) Schematic of configuration 12.

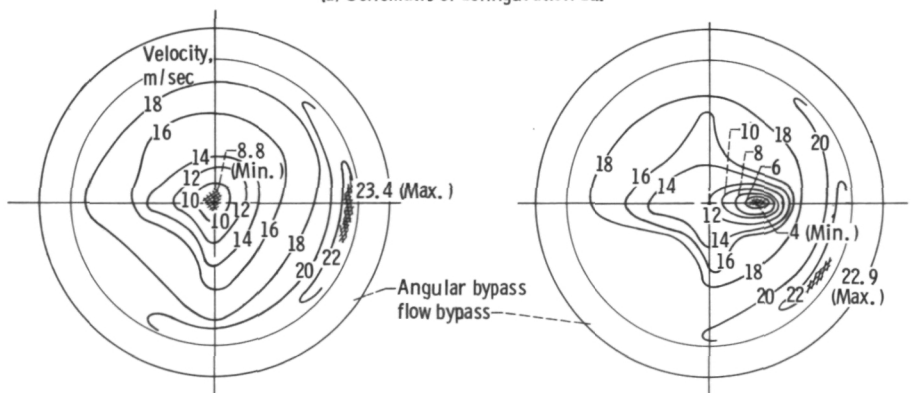

(b) Station 3 velocity pattern, looking downstream, without bypass flow; velocity spread, 14.6 meters per second.

(c) Station 3 velocity pattern, looking downstream, with 40-percent bypass flow; velocity spread, 18.9 meters per second.

Figure 18. - Schematic and performance of configuration 12 in PSL 3 inlet model with flow from atmospheric air inlets.

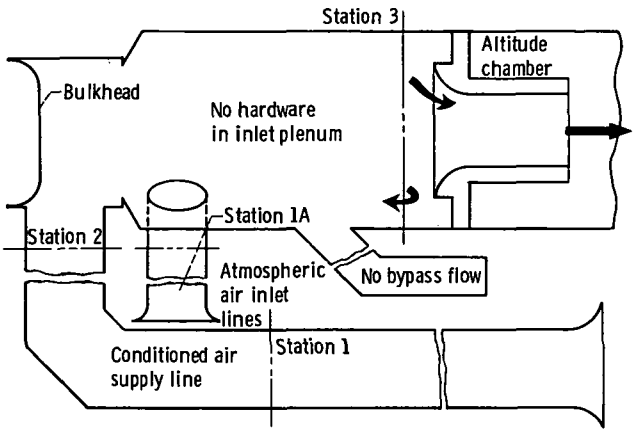

(a) Schematic of configuration 13.

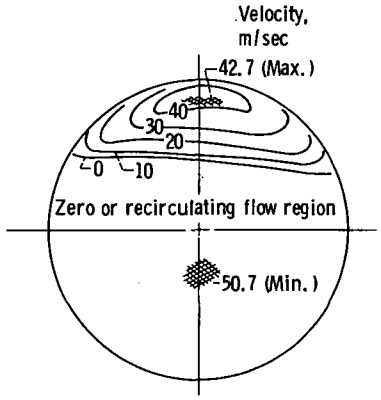

(b) Station 3 velocity pattern, looking downstream; conditioned inlet air; velocity spread, 93.4 meters per second (based on estimated negative velocities).

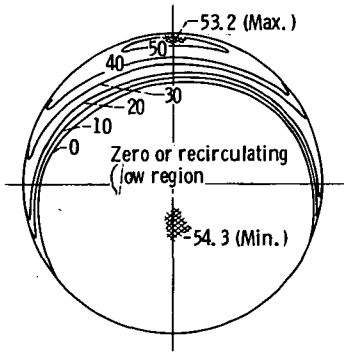

(c) Station 3 velocity pattern, looking downstream; atmospheric inlet air; velocity spread, 107.6 meters per second (based on estimated negative velocities).

Figure 19. - Schematic and performance of configuration 13 (plenum with no flow straightening hardware installed) in PSL 4 inlet model.

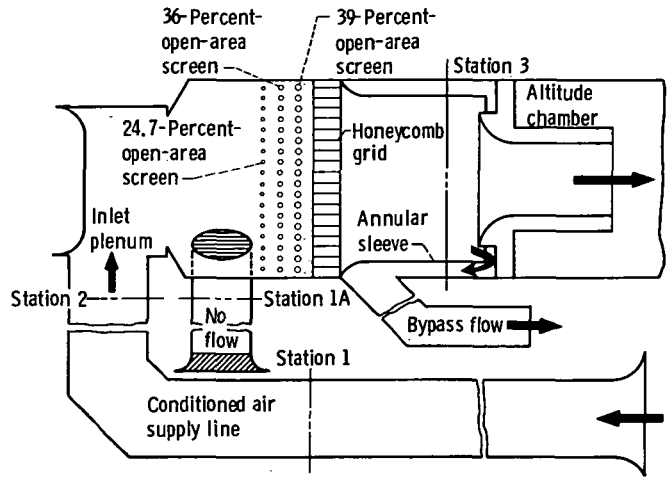

(a) Schematic of configuration 14.

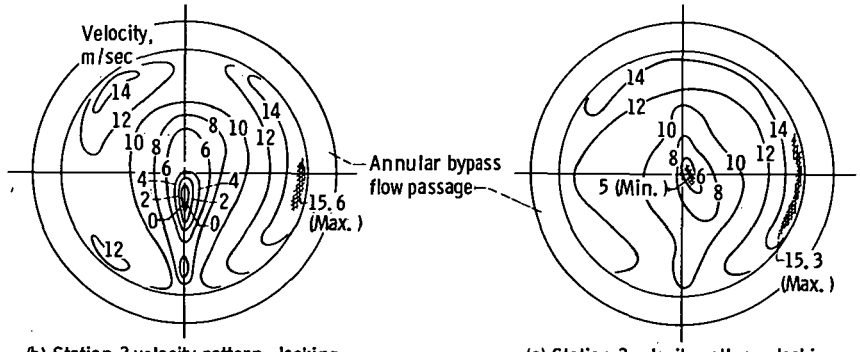

(b) Station 3 velocity pattern, looking downstream, with no bypass flow; velocity spread, 15.6 meters per second.

(c) Station 3 velocity pattern, looking downstream, with 40-percent bypass flow; velocity spread, 10.3 meters per second.

Figure 20. - Schematic and performance of configuration 14 in PSL 4 inlet model with conditioned inlet air.

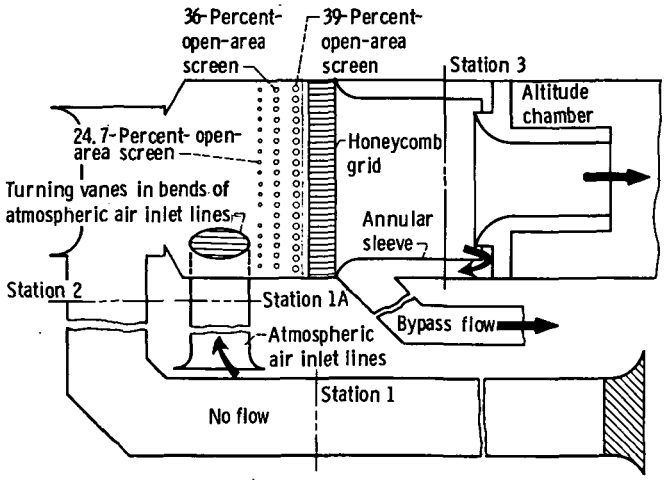

(a) Schematic of configuration 14.

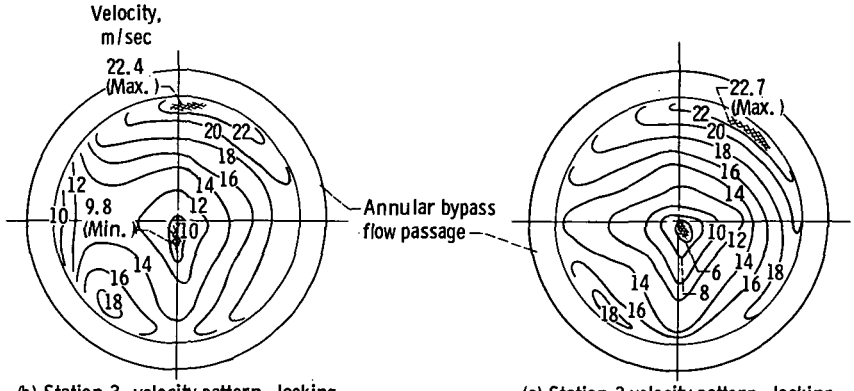

(b) Station 3, velocity pattern, looking downstream, with no bypass flow; velocity spread, 12.6 meters per second.

(c) Station 3 velocity pattern, looking downstream with 40-percent bypass flow; velocity spread, 16.7-meters per second.

Figure 21. - Schematic and performance of configuration 14 in PSL 4 model with atmospheric inlet air.

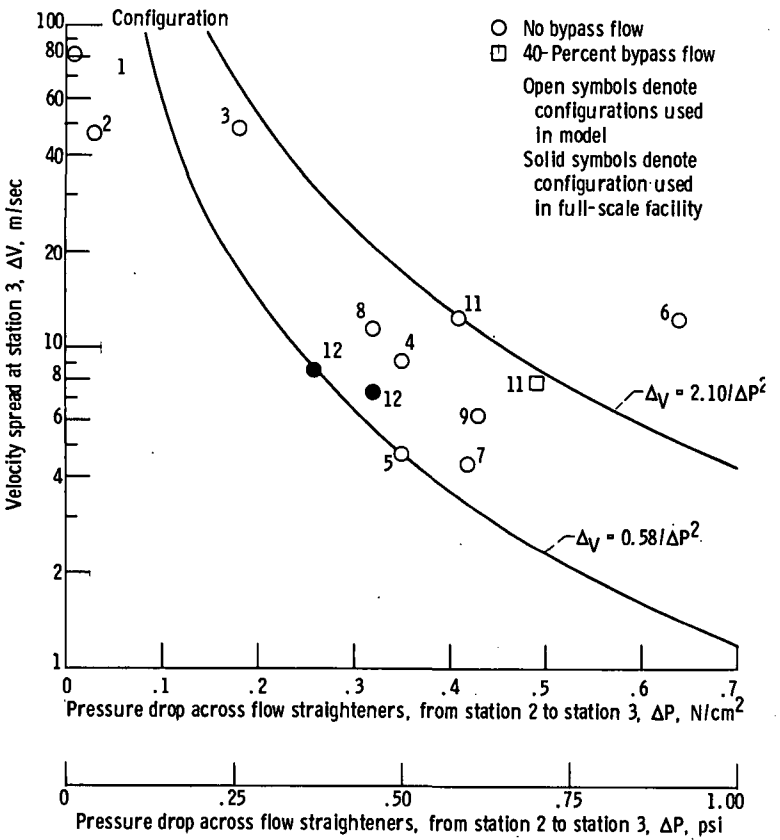

Figure 22. - Relation between velocity spread and pressure drop across flow straighening configurations in PSL 3 model. Conditioned inlet air; flow rate, 0.75 kilogram per second (1.65 lbm/sec).

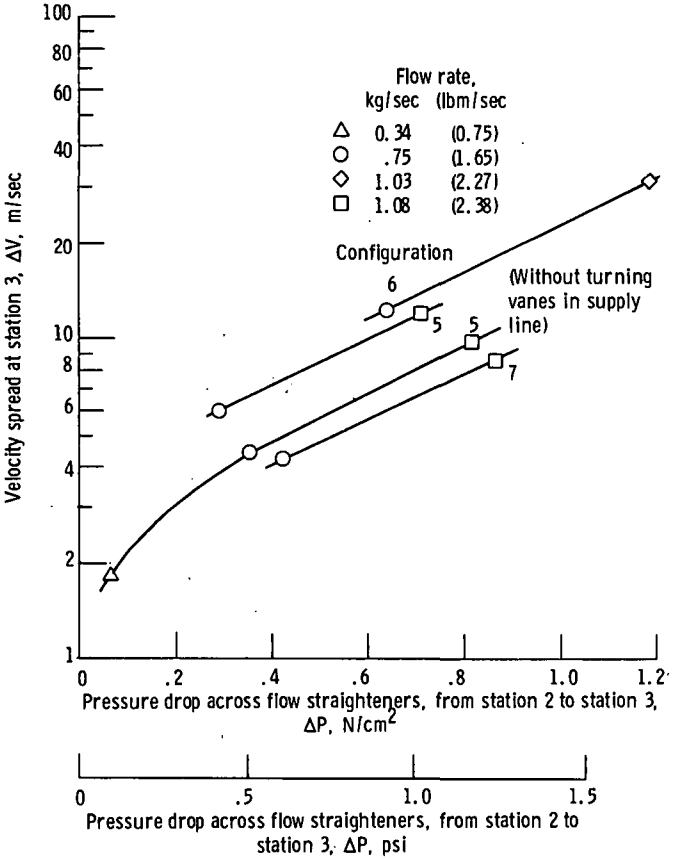

Figure 23. - Performance of various flow straightening configurations at different flow rates.

"The aeronautical and space activities of the United States shall be conducted so as to contribute . . . to the expansion of human knowledge of phenomena in the atmosphere and space. The Administration shall provide for the widest practicable and appropriate dissemination of information concerning its activities and the results thereof."

—NATIONAL AERONAUTICS AND SPACE ACT OF 1958

NASA SCIENTIFIC AND TECHNICAL PUBLICATIONS

TECHNICAL REPORTS: Scientific and technical information considered important, complete, and a lasting contribution to existing knowledge.

TECHNICAL NOTES: Information less broad in scope but nevertheless of importance as a contribution to existing knowledge.

TECHNICAL MEMORANDUMS: Information receiving limited distribution because of preliminary data, security classification, or other reasons. Also includes conference proceedings with either limited or unlimited distribution.

CONTRACTOR REPORTS: Scientific and technical information generated under a NASA contract or grant and considered an important contribution to existing knowledge.

TECHNICAL TRANSLATIONS: Information published in a foreign language considered to merit NASA distribution in English.

SPECIAL PUBLICATIONS: Information derived from or of value to NASA activities. Publications include final reports of major projects, monographs, data compilations, handbooks, sourcebooks, and special bibliographies.

TECHNOLOGY UTILIZATION PUBLICATIONS: Information on technology used by NASA that may be of particular interest in commercial and other non-aerospace applications. Publications include Tech Briefs, Technology Utilization Reports and Technology Surveys.

Details on the availability of these publications may be obtained from:

SCIENTIFIC AND TECHNICAL INFORMATION OFFICE

NATIONAL AERONAUTICS AND SPACE ADMINISTRATION

Washington, D.C. 20546